

**DETECTION OF OXYGEN IMPLANTATION VIA ELECTRON IRRADIATION OF WATER ICE ON SILICON USING AFM-IR TECHNIQUES.** C. E. Caplan<sup>1\*</sup>, G. Dominguez<sup>1</sup>, J. J. Gillis-Davis<sup>2</sup>, K. D. McKeegan<sup>3</sup>, and M. C. Liu<sup>3,4</sup>, <sup>1</sup>Physics Department, California State University, San Marcos, CA USA; <sup>2</sup>Washington University in St. Louis, Department of Physics, St. Louis, MO USA; <sup>3</sup>Dept. of Earth, Planetary, and Space Sciences, University of California, Los Angeles, CA USA, <sup>4</sup>Lawrence Livermore National Laboratory \*ccaplan@csusm.edu

**Introduction:** A few mechanisms have been proposed to explain the enrichment of <sup>17</sup>O and <sup>18</sup>O in planetary bodies compared to the Sun (e.g., nearby supernova injection of <sup>16</sup>O into the early solar system [1], self-shielding of CO [2-4]), but none have definitively explained this enrichment [5]. One model suggests that surface chemical interactions between oxygen bearing volatile compounds and dust grains may create <sup>17</sup>O and <sup>18</sup>O enriched grains [5-6].

Previous experiments and measurements with secondary ion mass spectroscopy (SIMS) showed that electron irradiation of water ice covered surfaces generated anomalous oxygen isotope exchange with the underlying surface [6]. This process created surface area averaged oxygen isotopic fractionations with slopes ranging from 0.96 to 1.11 on a triple isotope plot and with  $\Delta^{17}\text{O}$  values of -3.91 to 3.67 ‰ [6]. Here we report on a set of experiments with a goal of better understanding the uniformity of this isotope exchange under the experimental conditions probed.

We used Atomic Force Microscopy based-infrared spectroscopy (AFM-IR) to map the formation of Si-O bonds on Si surfaces to better understand the variability and magnitude of previous SIMS measurements.

**Methods:** Electron irradiation experiments were performed using the Isotope Characterization Experiment (ICE) at California State University San Marcos (CSUSM). A silicon wafer (Ted Pella) was cut into a 12.4 mm disk using a diamond drill bit. The sample was placed in a holder attached to a cryostat arm (ColdEdge) that was sealed into the Ultra-High-Vacuum chamber (UHV) pumped down to  $\sim 1 \times 10^{-8}$  Torr using a magnetically levitated turbo pump backed by an oil free scroll pump. The cryostat was set to 10 K. Greenland Ice Sheet Precipitation (GISP;  $\delta^{18}\text{O} = -24.78 \pm 0.09 \text{ ‰}$ ,  $\delta^{17}\text{O} = 0.52 \times \delta^{18}\text{O}$ ) was injected into an adjoining high vacuum line using a stainless-steel syringe. Water was deposited onto the cold silicon surface via a valve and stainless-steel pipe pointed directly at the sample within the UHV chamber.

Three types of experiments were performed: (1) water deposited and frozen onto silicon for three separate experiments before irradiation (named *pre-10*, *-25*, and *-50  $\mu\text{L}$* ). (2) water deposited onto the surface of one disk after irradiation, to determine if water needed to be simultaneously present for implantation (named *post-25  $\mu\text{L}$* ), and (3) a control irradiation experiment without water (named *Irradiation Only*).

The electron irradiation commenced when the UHV chamber stabilized to  $\sim 2 \times 10^{-8}$  Torr. A Kimball Physics electron gun was set to an energy of 5 keV and an emission of 50  $\mu\text{A}$ . The focus and deflectors were set to create a centered  $\sim 6$  mm diameter beam. The electron flux was monitored with data acquisition code in Matlab that utilized a Faraday cup and picoAmmeter. The experiment nominally would run at 50  $\mu\text{A}$  for 450 minutes, but the emission was not stable during experiments. The instability issue was overcome by ensuring each experiment experienced the same fluence (= emission  $\times$  time), which was done by recording the emission every 10 minutes. After electron irradiation, the cryostat was stopped, and the sample was brought to room temperature. The chamber was then vented and the sample was prepared for analysis.

Each experimental sample was analyzed using AFM-IR at CSUSM [7]. Various locations across the surface of each sample (from edge to center) were examined to understand sample heterogeneity. At each location, an AFM scan was taken to produce Height and IR Amplitude maps. The scans were taken at a rate of 0.5 Hz, with a 200-point resolution for 1-30  $\mu\text{m}^2$  regions. Within the scanned regions, point spectra (1931-915  $\text{cm}^{-1}$ ) were taken of the sample surface. Images of the height and IR Amplitude maps were flattened and scaled using Matlab.

**Results & Discussion:** Scans and point spectra of the five silicon experiments and a silicon blank (named *Silicon Standard*) were collected using the AFM-IR at CSUSM. Point spectra on the surface of each sample show the effects of electron irradiation on silicon wafers with or without water ice (Fig. 1). For the spectral range of this AFM-IR, evidence of oxygen implantation from these experiments would be expected by the presence of the Si-O-Si asymmetric stretch from 1200-1000  $\text{cm}^{-1}$ , dominantly around 1100  $\text{cm}^{-1}$  [8]. This peak is observed for each experiment with water ice deposition (pre-10, -25, -50  $\mu\text{L}$ , and post-25  $\mu\text{L}$ ), showing that Si may be oxidized by water (and its by-products) as a result of electron irradiation. For reference, the Silicon Standard and the Irradiation Only samples did not display a peak in this region, showing that water is needed for production of a Si-O-Si peak and that transient exposure to atmospheric oxygen (as H<sub>2</sub>O or O<sub>2</sub>) does not result in any detectable oxidation of the radiation damaged surface. Additionally, each water ice covered (exposed) sample shows a range of IR Ampli-

tudes at  $1100\text{ cm}^{-1}$ . This suggests heterogeneous oxygen implantation across sample surfaces, but more analyses are needed to understand the scale of heterogeneity.

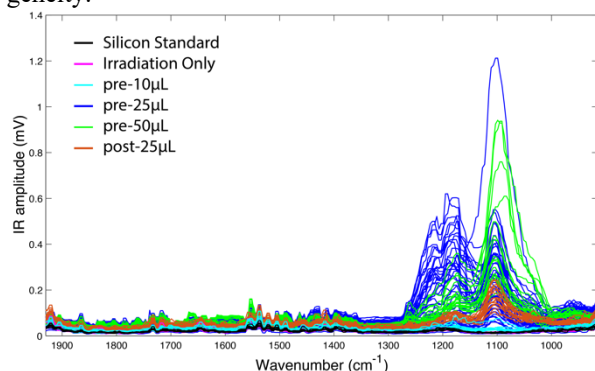


**Figure 1:** IR spectra taken with AFM-IR of silicon wafer irradiated experiments with varying quantities of water ice deposition (smoothed). Each spectrum is from a different location on the sample surface. The Silicon Standard spectra very closely overlaps the Irradiation Only spectra.

Further examination of the water deposited experiments show a possible relationship between the amount of water deposited and the IR Amplitude (Fig. 1). The pre-10  $\mu\text{L}$  sample shows the lowest IR Amplitude peak at  $1100\text{ cm}^{-1}$ , which is similar to the amplitude of the Silicon Standard and the Irradiation Only samples. This low amplitude may suggest a lower limit to the amount of water needed for oxygen implantation for this experimental setup. The pre-25  $\mu\text{L}$  and pre-50  $\mu\text{L}$  samples show higher amplitudes compared to the other samples in Fig. 1. For these two samples, a location on pre-25  $\mu\text{L}$  has the highest amplitude at  $1100\text{ cm}^{-1}$ , but the remaining spectra from this sample are lower than multiple spectra from the pre-50  $\mu\text{L}$  sample. The high spectral amplitude from the pre-25  $\mu\text{L}$  sample could be an anomaly, or it may suggest that additional locations on each sample need to be explored in future analyses. If the high amplitude from the pre-25  $\mu\text{L}$  sample is an anomaly, then the pre-50  $\mu\text{L}$  sample would have the highest amplitudes amongst the samples, suggesting that the quantity of water ice may influence the amount of oxygen that is exchanged between volatile ices and the refractory oxygen bearing surfaces underneath. A final experiment was performed to see if the addition of water ice after irradiation would produce similar spectral effects. The post-25  $\mu\text{L}$  sample showed defined peaks around  $1100\text{ cm}^{-1}$ , but the peak amplitude was lower than that of the pre-25  $\mu\text{L}$  sample. This difference in amplitude suggests that irradiation of a waterless surface followed by exposure to water ice could still induce isotope exchange, but not to the same extent as pre-deposited water ice.

Detailed AFM maps revealed that some regions

experienced extensive oxidation. For example, Figure 2 shows Height (A) and IR Amplitude (B) maps of two rod-like particles on the surface of the pre-25  $\mu\text{L}$  sample. These rods are above the sample surface (Fig. 2A) and they have higher IR Amplitudes than the sample surface (Fig. 2B). Point spectra show the low amplitude peak at  $1100\text{ cm}^{-1}$  for the surface spectra compared to the higher amplitude peaks of the rod-like particles ( $1175$  and  $1130\text{ cm}^{-1}$ ) (Fig. 2C). These particles were seen throughout the pre-25  $\mu\text{L}$  sample and in one location of the pre-50  $\mu\text{L}$  sample ( $\sim 1$  to  $12\text{ }\mu\text{m}$  in length for rods seen in scans). Rod-like particles were not observed on the Silicon Standard or the Irradiation Only sample, suggesting that processes during the water ice experiments may have produced these particles.

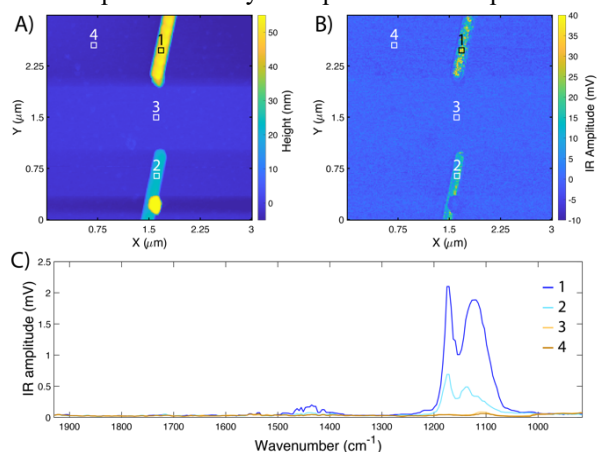


**Figure 2:** A) Height and B) IR Amplitude ( $1100\text{ cm}^{-1}$ ) maps of a region on the pre-25 $\mu\text{L}$  sample. The maps show two rod-shaped particles (full lengths of top and bottom rods are  $\sim 1$  and  $4\text{ }\mu\text{m}$ , respectively) on the surface of the sample. C) Point spectra (smoothed) for corresponding locations in Height and IR Amplitude maps.

Electron irradiation of water ice covered Si shows that oxidation (and therefore isotope exchange) can occur in cold astrophysical environments with similar conditions, such as permanently shadowed regions of the moon that are likely exposed to cosmic rays [9]. Future investigations of these samples will determine the overall heterogeneity of oxygen implantation at other electron energies to determine optimal experimental conditions for these types of experiments.

**References:** [1] Clayton R. N. et al. (1973) *Science*, 182, 485. [2] Clayton R. N. (2002) *Nature*, 415, 860. [3] Lyons J. R. and Young E. D. (2005) *Nature*, 435, 317. [4] Yurimoto H. and Kuramoto K. (2004) *Science*, 305, 1763. [5] Dominguez G. (2010) *ApJ Letters*, 713, L59. [6] Dominguez G. et al. (2019) *LPSC L*, Abstract # 2872. [7] Dazzi A. and Prater C. B. (2017) *Chemical Reviews*, 117, 5146. [8] Smith B. (2018) *CRC press*. [9] Li S. et al. (2018) *Proceedings of the National Academy of Sciences* 115, 8907. Supported by NASA grants 80NSSC19K1051 (GD) and SSERVI award NNA80NSSC20M0027 (JGD).